Ruthenium-Based Complexes Bearing Saturated Chiral N-Heterocyclic Carbene Ligands: Dynamic Behavior and Catalysis

Fabia Grisi,* Chiara Costabile, Emanuela Gallo, Annaluisa Mariconda, Consiglia Tedesco, and Pasquale Longo

Dipartimento di Chimica, Università di Salerno, Via Ponte Don Melillo, I-84084 Fisciano, Salerno, Italy

Received May 21, 2008

The synthesis of Ru-based catalysts, presenting saturated chiral C_2 symmetric (**3**, **5**) and C_1 symmetric (**4**) N-heterocyclic carbene (NHC) ligands bearing N-(*S*)-phenylethyl groups, was carried out. Variable-temperature NMR studies were conducted to investigate the interconversion of atropisomers in solution. The complex behaviors were rationalized evaluating the rotation barrier of alkylidene and NHC groups around the C−Ru bonds, by DFT calculations. Comparison between NMR data and DFT calculations suggested that interconversion between different atropisomers, which occurs at room temperature, is due to the free rotation of the benzylidene group around the Ru=C bond. The activity and stereoselectivity of **3**−**5** were investigated in ring-closing metathesis (RCM), asymmetric ring-closing metathesis (ARCM), cross-metathesis (CM), and ring-opening metathesis polymerization (ROMP). **4** showed the highest activity in all reactions and gave a significantly low *E:Z* ratio in the CM reaction. Modest enantioselectivity in the ARCM of an achiral triene was observed in the presence of C_2 symmetric catalyst **5**.

Introduction

The last decades have seen olefin metathesis emerging as one of the most useful methods for constructing C=C bonds.[1] Since the discovery of well-defined Ru alkylidene complexes able to catalyze olefin metathesis reactions,[2] (**1** of Chart 1) intensive research efforts were devoted to the synthesis of more efficient catalytic precursors, culminating in the substitution of one posphine ligand with an N-heterocyclic carbene (NHC) ligand (**2**).[3,4] In addition to the increased stabilization determined by the enhanced σ-donor properties, the NHC ligand offers the advantage to fine-tune the catalyst properties by modifying the backbone and N-substituents. A large number of both NHC ligands and corresponding Ru complexes, bearing aromatic amino side groups, is well known to be of easy preparation and of high stability. Nevertheless, many efforts were made in order to introduce N-aliphatic groups to improve the catalytic performances of the resulting catalysts. In fact, an enhancement of the activity is generally expected from the presence of more electron-donating N-alkyl substituents. Further increase of activity is postulated for the same reason for saturated NHCs compared to their unsaturated analogues. To the best of our knowledge, symmetrical dihydro NHC ligands are limited to aromatic N-substituents.[3,5] Metathesis complexes bearing N-alkyl-N-mesityl unsymmetrical NHCs have been reported by Mol, Blechert, Collins, and Verpoort.[6,7]

Recently, a variety of chiral Ru catalysts, active in asymmetric olefin metathesis, were developed. In particular, Ru catalysts with monodentate NHC ligands presenting a chiral backbone have been shown to be very active and to give high enantioselectivities in the asymmetric ring-closing metathesis (ARCM).[8,9] On the contrary, due to a poor transfer of the asymmetric information,[10] NHC-Ru catalysts characterized by N-chiral substituents generally exhibit only modest selectivity in ARCM[8] and not significantly different selectivity compared to achiral catalysts in asymmetric ring-opening metathesis polymerization (AROMP).[11]

Herein, we report synthetic, structural, and catalytic studies of Ru-based complexes bearing monodentate saturated symmetrical NHC ligands with phenylethyl N-substituents. The replacement of aromatic rings on nitrogen atoms with more electron-donating and differently sterically demanding benzyl-type groups can significantly influence the NHCs' properties. Consequently, the effect of the changed electronic and steric properties of the resulting catalysts on metathesis activity and selectivity has been investigated. Moreover, modifying the NHC ligand by introducing chirality both at nitrogen and on the carbone backbone, it has been possible to obtain valuable

* Corresponding author. E-mail: fgrisi@unisa.it.

(1) (a) Füstner, A. *Angew. Chem.* **2000**, *112*, 3140; *Angew. Chem. Int. Ed.* **2000**, *39*, 3012. (b) Grubbs, R. H. *Handbook of Olefin Metathesis*; Wiley-VCH: Weinheim, 2003. (c) Schrock, R. R.; Hoveyda, A. H. *Angew. Chem.* **2003**, *115*, 4740; *Angew. Chem., Int. Ed.* **2003**, *42*, 4592.

(2) (a) Nguyen, S. T.; Grubbs, R. H.; Ziller, J. W. *J. Am. Chem. Soc.* **1993**, *115*, 9858. (b) Schwab, P.; Grubbs, R. H.; Ziller, J. W. *J. Am. Chem. Soc.* **1996**, *118*, 100.

(3) Scholl, M.; Ding, S.; Lee, C. W.; Grubbs, R. H. *Org. Lett.* **1999**, *1*, 953.

(4) (a) Scholl, M.; Trnka, T. M.; Morgan, J. P.; Grubbs, R. H. *Tetrahedron Lett.* **1999**, *40*, 2247. (b) Huang, J.; Stevens, E. D.; Nolan, S. P.; Peterson, J. L. *J. Am. Chem. Soc.* **1999**, *121*, 2674. (c) Weskamp, T.; Kohl, F. J.; Hieringer, W.; Gliech, D.; Herrman, W. A. *Angew. Chem.* **1999**, *111*, 2573; *Angew. Chem., Int. Ed.* **1999**, *38*, 2416. (d) Morgan, J. P.; Grubbs, R. H. *Org. Lett.* **2000**, *2*, 3153.

(5) Dinger, M. B.; Mol, J. C. *Adv. Synth. Catal.* **2002**, *344*, 671.

(6) (a) Dinger, M. B.; Nieczypor, P.; Mol, J. C. *Organometallics* **2003**, *22*, 5291. (b) Vehlow, K.; Maechling, S.; Blechert, S. *Organometallics* **2006**, *25*, 25. (c) Fournier, P.-A.; Collins, S. K. *Organometallics* **2007**, *26*, 2945. (d) Vehlow, K.; Wang, D.; Buchmeiser, M. R.; Blechert, S. *Angew. Chem.* **2008**, *120*, 2655; *Angew. Chem., Int. Ed.* **2008**, *47*, 1.

(7) Ledoux, N.; Allaert, B.; Pattyn, S.; Mierde, H. V.; Vercaemst, C.; Verpoort, F. *Chem.−Eur. J.* **2006**, *12*, 4654.

(8) Seiders, T. J.; Ward, D. W.; Grubbs, R. H. *Org. Lett.* **2001**, *3*, 3225.

(9) Funk, T. W.; Berlin, J. M.; Grubbs, R. H. *J. Am. Chem. Soc.* **2006**, *128*, 1840.

(10) Costabile, C.; Cavallo, L. *J. Am. Chem. Soc.* **2004**, *126*, 9592.

(11) Hamilton, J. G.; Frenzel, U.; Kohl, F. J.; Weskamp, T.; Rooney, J. J.; Herrmann, W. A.; Nuyken, O. *J. Organomet. Chem.* **2000**, *606*, 8.

10.1021/om800459y CCC: $40.75
Publication on Web 08/19/2008

Chart 1

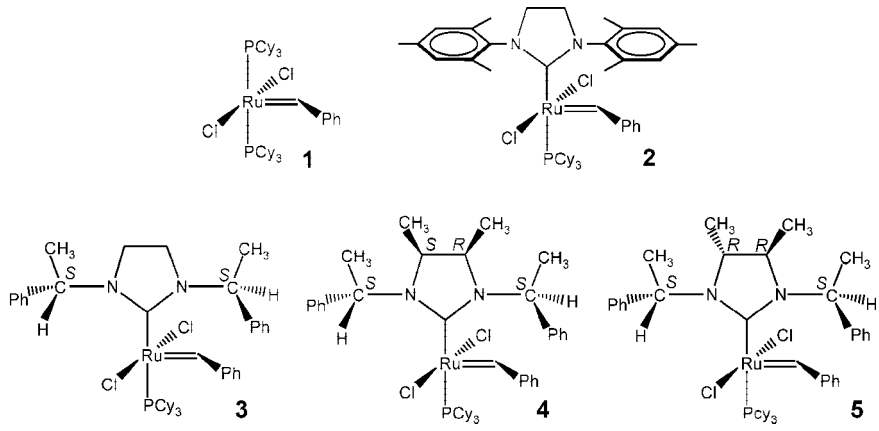

information about the correlation between the stereo chemical ligand architecture of the Ru complexes and the outcome of a catalytic metathesis process.

Results and Discussion

Synthesis and Characterization of 3−5. Synthesis of the ligand precursors began with the preparation of chiral diamines **6**−**8** of Scheme 1,[12] followed by their condensation with triethyl orthoformate and ammonium tetrafluoroborate to give the corresponding 4,5-dihydroimidazolium salts **9**−**11**.[13] These salts were treated with potassium hexafluoro-*tert*-butoxide and $(PCy)_3(Cl)_2Ru{=}CHPh$ to afford the desired chiral complexes **3**−**5** in around 40% yield.[9]

For the determination of the absolute stereochemistry, crystals of diamine **7** and imidazolinium salt **11** suitable for X-ray characterization were grown from ethyl acetate and cold ethanol, respectively.[14]

The ruthenium complexes were fully characterized by ^{1}H, ^{13}C, and ^{31}P NMR experiments (Table 1).

All these complexes exhibited characteristic signals in the ^{1}H NMR spectra, showing slightly downfield shifted singlets for the benzylidene protons compared to the signal for **2** of Chart 1. NMR diagnostic data trends do not provide enough elements to assume a high electron density at the carbenic center (arising from the presence of these nonaromatic N-substituents) that could have a positive effect on the catalytic activity of the corresponding NHC-Ru complexes.[15]

^{1}H and ^{31}P NMR experiments at variable temperature showed that both **4** and **5** present atropisomers. In particular, at low temperature **4** and **5** are characterized by the presence of four and two different isomers, respectively, while at room temperature the presence of only two and one isomer is revealed for **4** and **5**, respectively (Figure 1). The coalescence of the diagnostic peaks is indicative of the interconversion of atropisomer couples on the NMR time scale. In order to rationalize the dynamic behavior in solution, all possible isomers of **4** and **5** were modeled and energy barriers for their interconversions were obtained by DFT calculations.

Molecular Modeling Studies. Models and Nomenclature. In order to describe the modeled structures it is useful to define the dihedral angles θ and ϕ reported in Figure 2. θ, which is the dihedral angle C5−C4−Ru3−C2, defines the orientation of the alkylidene group with respect to the NHC ligand. As an example, $\theta = |90°|$ corresponds to the plane of the alkylidene group being perpendicular to the Ru−NHC bond axes. ϕ, which is the dihedral angle N1−C2−Ru3−C4, defines the orientation of the imidazolinium plane with respect to the Ru=C bond. As an example, $\phi = 0°$ or 180° corresponds to having the NHC ring in the same plane of the R=C axes.

The modeled structures were labeled, for example, **4ab**+$\theta^{\ddagger}$ with the following meaning: **4** corresponds to complex **4** of Chart 1, **a** and **b** are two of the minimum energy structures of complex **4**, and +$\theta^{\ddagger}$ corresponds to the transition state for the clockwise rotation of the alkylidene group around the Ru=C axes. Hence, in summary **4ab**+$\theta^{\ddagger}$ is the transition state for the clockwise rotation of the alkylidene group around the Ru=C axes from the minimum energy geometry **4a** to **4b**.

Results. All results relative to internal energies and free energies in gas and solvent (CH_2Cl_2, toluene) phase are collected in Table 2. As for **4**, four minimum energy structures (**4a**, **4b**, **4c**, and **4d**) were located, and the corresponding geometries are shown in Figure 3. Both **4a** and **4b** present $\phi \approx 180°$ and differ in the θ angle, which is 100° and −90° for **4a** and **4b**, respectively. As for **4c** and **4d**, θ is 104° and −94°, respectively, whereas they both present ϕ close to 0°.

Internal energies of all four geometries are very similar, whereas **4d** presents a free energy in gas, CH_2Cl_2, and toluene

(12) (a) Bambridge, K.; Begley, M. J.; Simpkins, N. S. *Tetrahedron Lett.* **1994**, *35*, 3391. (b) Roland, S.; Mangeney, P.; Alexakis, A. *Synthesis* **1999**, *2*, 228. (c) Equey, O.; Alexakis, A. *Tetrahedron: Asymmetry* **2004**, *15*, 1069.

(13) Saba, S.; Brescia, A. M.; Kaloustain, M. K. *Tetrahedron Lett.* **1991**, *32*, 5031.

(14) Crystallographic data (excluding structure factors) for the structures reported in this paper have been deposited with the Cambridge Crystallographic Data Centre as supplementary publications nos. CCDC-680900 (compound **7**) and CCDC-680901 (compound **11**). Copies of data can be obtained free of charge from The Cambridge Crystallographic Data Centre via www.ccdc.cam.ac.uk/data_request/cif. For compound **7**, the torsion angles N1C1C2N2 and C3C1C2C4 are−61,74(5)° and 62.3(4)°, respectively, with the N amine atoms and the methyl groups in a *gauche* conformation. The phenyl moieties are almost perpendicular to each other with an angle of 82.9(1)° between the corresponding aromatic planes. For compound **11** a crystallographic 2-fold axis passes through the C1 atom; thus the molecular 2-fold symmetry is retained also in the crystals. The five-atom ring and the phenyl moieties are planar within a rmsd of respectively 0.013 and 0.006 Å; they are almost perpendicular to each other, the angle between the two planes being 84.5(1)°. The torsion angle C5−C4−C6−C11 is−92.0(4)°.

(15) (a) Viciu, M. S.; Navarro, O.; Germananeau, R. F.; Kelly, R. A., III.; Sommer, W.; Marion, N.; Stevens, E. D.; Cavallo, L.; Nolan, S. P. *Organometallics* **2004**, *23*, 1629. (b) Dorta, R.; Stevens, E. D.; Scott, N. M.; Costabile, C.; Cavallo, L.; Hoff, C. D.; Nolan, S. P. *J. Am. Chem. Soc.* **2005**, *127*, 2485. (c) Cavallo, L.; Correa, A.; Costabile, C.; Jacobsen, H. *J. Organomet. Chem.* **2005**, *690*, 5407.

Scheme 1. Synthetic Pathway toward 4,5-Dihydroimidazolium Salts 9−11

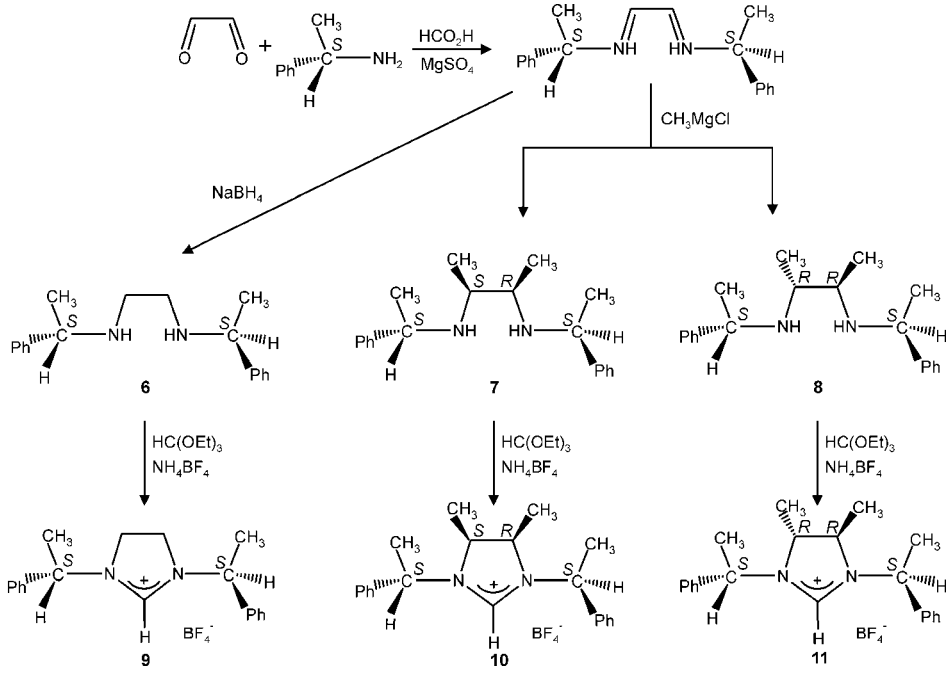

Table 1. Selected ^{1}H, ^{13}C, and ^{31}P NMR Data[a]

complex	$^{1}H_{alkylidene}$	$^{13}C_{NHC}$	$^{13}C_{alkylidene}$	^{31}P
1	20.02		294.72	36.6
2	19.16	220.3	294.24	31.4
3	20.04	214.9	291.06	39.0
4	20.03[b]	218.6	290.38	39.5
5	19.92	217.5	289.75	39.7

[a] Chemical shifts are given in ppm and measured in CD_2Cl_2. [b] Chemical shift of the major isomer.

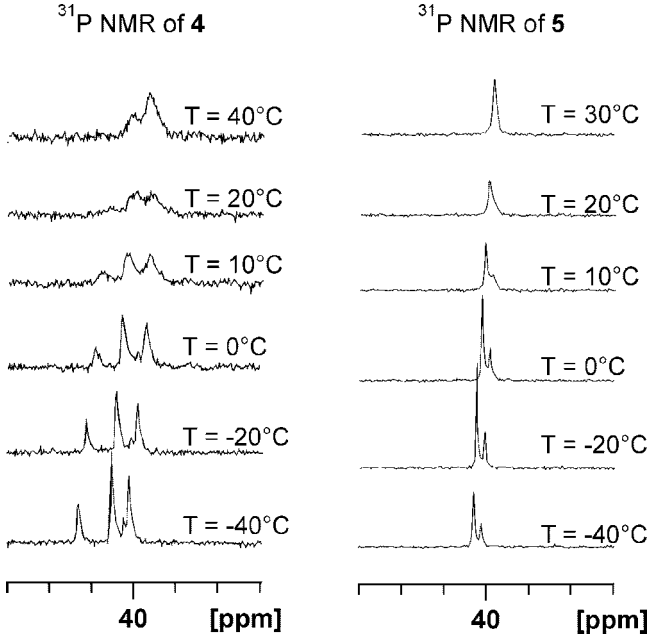

Figure 1. ^{31}P NMR spectra of **4** and **5** at variable temperature.

phase higher than all other geometries (3.9, 5.7, and 5.1 kJ/mol with respect to **4a**, respectively).

Structure **4a** can isomerize to **4b** by rotation of the alkylidene group around θ. The same isomerization can occur between **4c** and **4d**. Furthermore, an isomerization of **4a** to **4c**, as well as of **4b** to **4d**, can occur through rotation of NHC around ϕ (see Scheme 2). Moreover, all isomerizations can, in principle, occur through clockwise or counterclockwise rotations. In order to evaluate the energy barriers for the reported isomerization reactions, starting from **4a**, all transition state energies relative to the rotation of the alkylidene group around θ, and of NHC around ϕ, leading to **4b** and **4c**, respectively, were calculated. We assumed that the energy barriers for the isomerization of **4c** to **4d** and of **4b** to **4d** would be comparable to that of **4a** to **4b** and of **4a** to **4c**, respectively, and, as a consequence, they were not calculated.

Transition state geometries are shown in Figure 4. Structures **4ab-$\theta^{\ddagger}$** and **4ab+$\theta^{\ddagger}$** correspond to transition state geometries relative to the rotation of the alkylidene group, and their energy and free energy are collected in Table 2. Results indicate that, starting from **4a**, a counterclockwise rotation of the alkylidene group (**4ab−$\theta^{\ddagger}$**) is favored with respect to a clockwise rotation (**4ab+$\theta^{\ddagger}$**). Indeed, the internal energy difference between this two structures is 23 kJ/mol, whereas the free energy difference is lower, especially in the solvent phase (about 8 kJ/mol in toluene). Structures **4ac+$\phi^{\ddagger}$** and **4ac-$\phi^{\ddagger}$**, corresponding to the transition state geometries of the NHC group, present internal energies at least 40 kJ/mol higher than **4ab−$\theta^{\ddagger}$** (see Table 2). Indeed, the most favored transition state geometry for the NHC group rotation, **4ac+$\phi^{\ddagger}$**, presents high steric interactions between the NHC group and the Cl atoms, whereas the alkylidene group of **4ab−$\theta^{\ddagger}$** minimizes its steric interactions with the PCy_3 ligand by rotating the aromatic ring. In fact, dihedral angle C6−C5−C4−Ru3 of **4ab−$\theta^{\ddagger}$** (Figure 2) is about −90°, whereas in all the minimum energy species it is close to 0°. For an easy understanding, a simplified model is sketched in Chart 2.

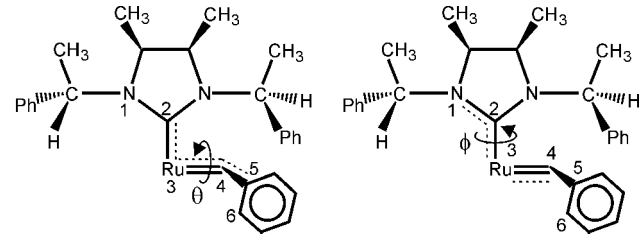

Figure 2. Definition of the dihedral angles θ and ϕ.

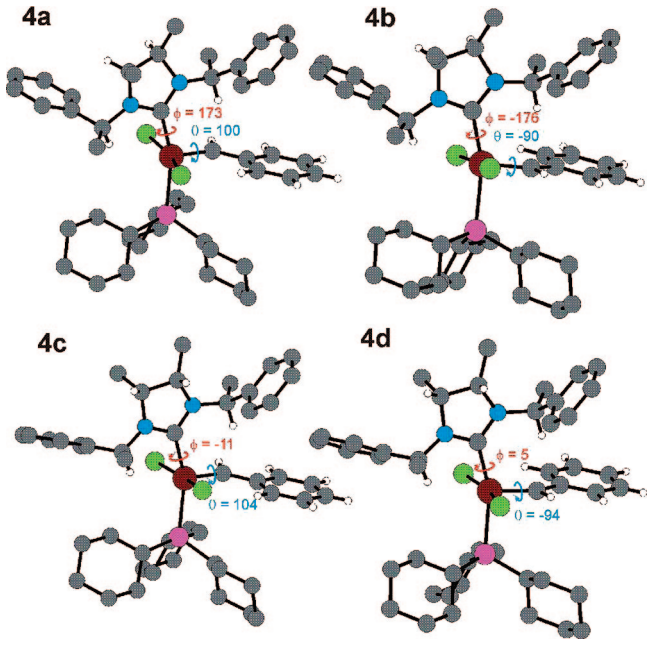

Figure 3. Minimum energy structures of complex **4**.

Scheme 2. Interconversions between Isomers of 4 and 5

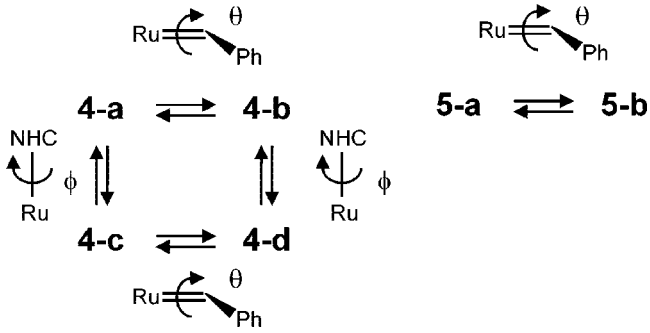

In Figure 5, the two minimum energy structures, located for the C_2 symmetric complex **5**, **5a** and **5b**, are shown. θ is 102° and −96° for **5a** and **5b**, respectively. Due to the symmetry of the NHC ligand, $\phi \approx 0°$ and $\phi \approx 180°$ would give the same isomeric structure. For this reason the rotational barrier of the NHC group around Ru−C was not evaluated.

The most favored calculated internal energy barrier, starting from **5a**, and corresponding to **5ab**−$\boldsymbol{\theta}^{\ddagger}$ (see structure in Figure 6), is 63.0 kJ/mol. The free energy barrier calculated in CH_2Cl_2 is 60.0 kJ/mol.

The calculated value was compared with the free energy barrier estimated by ^{31}P NMR spectra in CD_2Cl_2 and by using

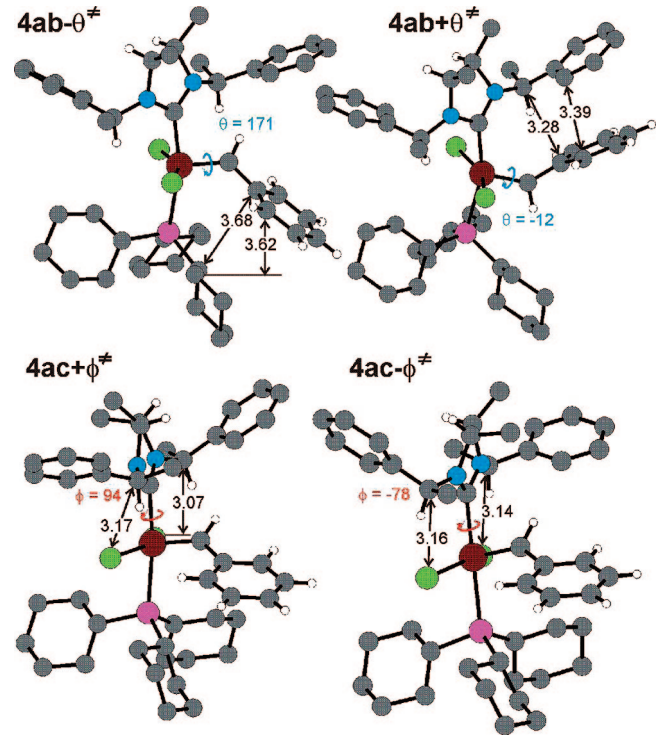

Figure 4. Transition states, from minimum energy strucure **4a** to **4b**, relative to counterclockwise (**4ab**−$\boldsymbol{\theta}^{\ddagger}$) and clockwise (**4ab**+$\boldsymbol{\theta}^{\ddagger}$) rotation around θ, and from **4a** to **4c** relative to clockwise (**4ac**+$\phi^{\ddagger}$) and the counterclockwise (**4ac**−$\phi^{\ddagger}$) rotation aroud ϕ.

Chart 2

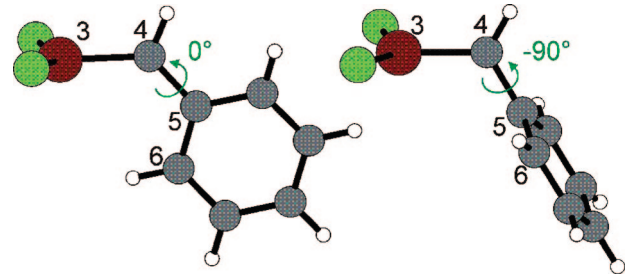

the Eyring plot of the corresponding rates of interconversion, obtained by line shape simulations (for details see the Supporting Information). The free energy of activation for the interconversion of the two isomers of complex **5** at 25 °C is $\Delta G^{\ddagger} = 59 \pm 4$ kJ/mol, in excellent agreement with the calculated barrier correponding to the alkylidene rotation.

Comparison between DFT calculations and NMR experiments, conducted in CD_2Cl_2, leads to the following conclusions:

Table 2. Energies[a] and Relevant Geometric Parameters of the Discussed Species

system	*E*	*G*	$G_{(CH2Cl2)}$	$G_{(Tol)}$	θ	ϕ
4a	0	0	0	0	100.3	173.3
4b	0.4	−1.8	−4.4	−4.8	−90.0	−176.4
4c	2.5	0.6	0.5	0.7	104.4	−11.4
4d	0.5	3.9	5.7	5.1	−94.7	5.1
4ab−$\boldsymbol{\theta}^{\ddagger}$	43.3	45.4	52.7	49.2	171.2	143.5
4ab+$\boldsymbol{\theta}^{\ddagger}$	65.1	58.7	61.7	57.6	−12.8	−156.9
4ac+$\phi^{\ddagger}$	83.4	85.7	90.4	85.9	137.3	94.3
4ac−$\phi^{\ddagger}$	100.3	100.8	106.1	104.1	138.8	−78.2
5a	0	0	0	0	101.8	172.2
5b	−2.1	0.2	3.0	2.5	−95.9	−166.1
5ab−$\boldsymbol{\theta}^{\ddagger}$	63.0	68.4	60.0	57.0	−173.0	145.4
5ab+$\boldsymbol{\theta}^{\ddagger}$	67.8	69.1	66.9	63.3	−7.9	−167.3

[a] In kJ/mol.

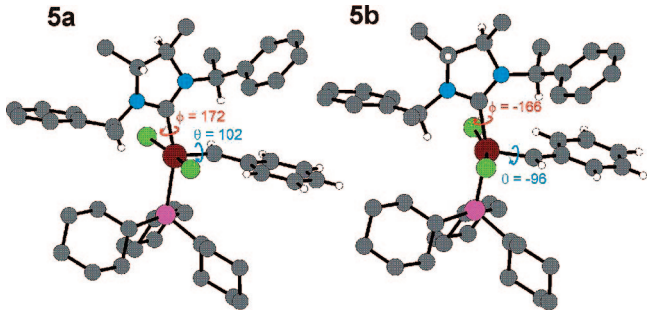

Figure 5. Minimum energy structures of complex **5**.

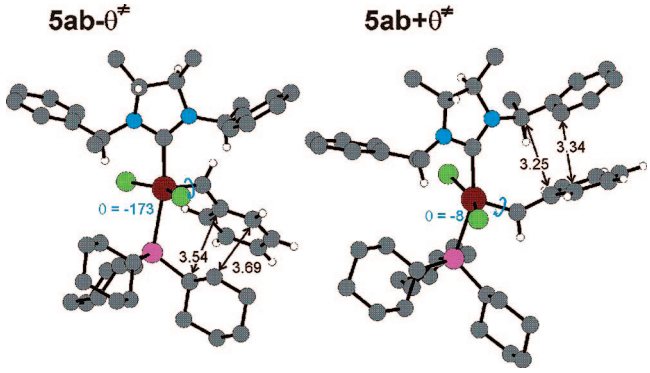

Figure 6. Transition states, from minimum energy strucure **5a** to **5b**, relative to counterclockwise (**5ab**$-\theta^{\neq}$) and clockwise (**5ab**$+\theta^{\neq}$) rotation around θ.

• Low-temperature NMR experiments reveal the presence of four isomers of complex **4**. According to DFT calculations, there are one favored isomer structure (**4b**) and two isomers with slightly higher energy (**4a** and **4c**), whereas the fourth isomer (**4d**) seems to be unfavored, and, as a consequence, we observe experimentally a lower population for one of the isomers, which should correspond to **4d**.

• The calculated free energy barrier in CH_2Cl_2 to promote the isomerization of **4a** to **4b** is 52.7 kJ/mol, whereas that of **4a** to **4c** is 90.4 kJ/mol. These energy values are in agreement with the experimental observed coalescence of four isomers in two isomers by increasing the temperature. In fact we can assume that the interconversion between **4a** and **4b** (as well as **4c** and **4d**) occurs faster than NMR time scale at room temperature. On the other hand, the isomerization of **4a** to **4c** (as well as **4b** to **4d**) is too unfavored, and this can explain the presence of two NMR diagnostic peaks even at higher temperatures (as also shown by VT-NMR experiments conducted in toluene).

• Finally, low-temperature NMR experiments show the presence of two isomers of complex **5**. The calculated free energies of **5a** to **5b** are very close ($\Delta G_{CH2Cl2} = 3.0$ kJ/mol) and the barrier for the isomerization through alkylidene rotation ($\Delta G^{\ddagger}_{CH2Cl2} = 60.0$ kJ/mol) is slightly higher than the corresponding isomerization from **4a** to **4b** ($\Delta G^{\ddagger}_{CH2Cl2} = 52.7$ kJ/mol). $\Delta G^{\ddagger}$ experimental activation barrier for complex **5**, corresponding to 59 kJ/mol, is in excellent agreement with the calculated barrier correponding to the alkylidene rotation. Thus, DFT results are able to rationalize the NMR observed coalescence, from two to one isomer of **5**, below room temperature.

Catalytic Behavior. As a preliminary evaluation of the catalytic behavior of the newly synthesized complexes, **3**−**5** were tested in some diagnostic reactions reported by Grubbs et al.[16]

In the ring-opening metathesis polymerization (ROMP) of cyclooctadiene (**12**), monitored by ^{1}H NMR (see Table 3 and Figure 7), all the catalysts, under standard conditions,[16] disclosed high activities; for example, after 30 min, **4** gave a 99% conversion to poly(**12**).

^{1}H and ^{13}C NMR spectroscopy allowed the determination of the *Z* fraction of the newly formed double bond in the polymer chains. When complete conversions of **12** were achieved, the percentage of olefin with *Z* configuration in the resulting polymers is 64% for **3**, 55% for **4**, and 61% for **5** (entries 1−3, Table 3).

It is worth pointing out that generally Grubbs second-generation catalysts give rise to a polyalkenamer with a predominately *E* olefin content, as a consequence of an equilibrium-controlled polymerization in which secondary chain transfer occurs.[17]

On the other hand, first-generation catalyst leads to a higher *Z* olefin content, but it is also dramatically less active. Therefore, **3**−**5** show a very interesting behavior, giving conversions comparable to those of most Grubbs second-generation-like catalysts, but percentages of *Z* olefin in the polyalkenamer are very similar to those obtained in the presence of first-generation catalysts.[7,16]

Moreover, from monitoring the ROMP reaction by ^{1}H NMR it is evident that the *E:Z* ratio begins significantly to change when the conversion of **12** to the corresponding polymer is higher than 75%, indicating that secondary metathesis on existing polymer chains is strongly competitive with the growing of polymer chains, and it prevails when the concentration of monomer becomes too low. After complete conversion of **12**, it can be observed that the catalysts still work to isomerize the double bonds of the polymer chains from *Z* to *E*.[17]

The RCM efficiency of catalysts **3**−**5** was tested on the standard RCM substrate diethyl diallylmalonate (**13**) at 30 °C. The course of reaction was monitored by ^{1}H NMR spectroscopy, and the conversion of starting material to product (**14**) over time was measured and sketched in Figure 8.

Complexes **3**−**5** displayed modest activities in comparison with those of Grubbs first- and second-generation-like catalysts.[7,16] When the RCM reactions were performed at 40 °C, complex **4** reached 27% conversion in 1 h, while complexes **3** and **5** reached 20% and 22% conversions, respectively (entries 4−6, Table 3). As for the ROMP reaction, catalyst **4** showed the highest activity. The presence of substituents in positions 4 and 5 of the dihydroimidazole ring seems to increase the NHC ruthenium complex efficiency. Further the relative steric arrangement of the phenylethyl groups on nitrogen atoms and methyl groups on the carbon backbone in complex **4** could play a significant role in the formation of a more active productive species both in ROMP and in RCM reactions with respect to catalyst **5**.

We next investigated the activity of **3**−**5** in the representative cross-metathesis reaction of allyl benzene (**15**) and *cis*-1,4-diacetoxy-2-butene (**16**), represented in Scheme 3.[18] All the catalysts showed conversions to desired heterocoupled product **17** comparable to the Grubbs first- and second-generation catalysts and unexpected pronounced selectivity toward the formation of the *Z* isomer, up to an *E:Z* ratio 2.6:1 obtained with catalyst **4** (entry 8, Table 3). The rationalization of selectivity effects is currently under investigation.

A logical extension of our investigations was the application of **3**−**5** in asymmetric metathesis reactions.

Ru complexes of chiral imidazolin-2-ylidene ligands possessing stereogenic centers on the N-substituents were prece-

Table 3. ROMP, RCM, CM, and ARCM Conducted in the Presence of 3−5

entry	cat.	substrate	product	*t* (h)	yield, %[a]	*E*:*Z*[b]	ee[c]
1[d]	**3**	**12**	poly(**12**)	1	100	0.56	
2[d]	**4**	**12**	poly(**12**)	1	100	0.82	
3[d]	**5**	**12**	poly(**12**)	1	100	0.64	
4[e]	**3**	**13**	**14**	1	20		
5[e]	**4**	**13**	**14**	1	27		
6[e]	**5**	**13**	**14**	1	22		
7[f]	**3**	**15**−**16**	**17**	12	65[g]	4.2	
8[f]	**4**	**15**−**16**	**17**	12	70[g]	2.6	
9[f]	**5**	**15**−**16**	**17**	12	62[g]	4.6	
10[h]	**3**	**18**	**19**	2	66		4(*R*)
11[h]	**4**	**18**	**19**	2	100		-
12[h]	**5**	**18**	**19**	2	59		33(*R*)
13[i]	**5**	**18**	**19**	2	60		33(*R*)
14[j]	**5**	**18**	**19**	2	93		7(*S*)

[a] Determined by NMR. [b] Ratio based on data from ^{1}H and ^{13}C NMR of isolated products. [c] Determined by chiral GC. [d] Reaction conducted in CD_2Cl_2, at 30 °C, **3**−**5** 0.1 mol %, **12** 0.5 M.[16] [e] Reaction conducted in CD_2Cl_2, at 40 °C, **3**−**5** 1 mol %, **13** 0.1 M.[16] [f] Reaction conducted in CH_2Cl_2, at 40 °C, **3**−**5** 2.5 mol %, **15**−**16** 0.2 M.[18] [g] Yields from isolated products. [h] Reaction conducted in CD_2Cl_2, at 40 °C, **3**−**5** 2 mol %, **18** 0.055 M.[9] [i] Reaction conducted in CD_2Cl_2, at 40 °C, **3**−**5** 2.5 mol %, **18** 0.12 M, 0.1 equiv of 2,6-dichloro-1,4-benzoquinone.[23] [j] Reaction conducted in THF-d_8, at 40 °C, **3**−**5** 4 mol %, 25 equiv of NaI, **18** 0.055 M (after stirring **3**−**5** in solution with NaI for 1 h at RT).[9]

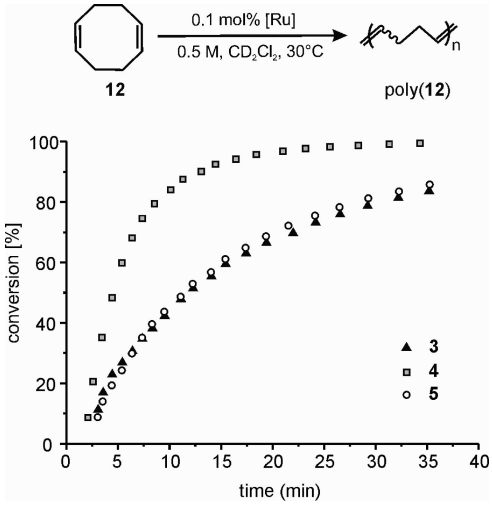

Figure 7. Monitoring ROMP of COD by ^{1}H NMR spectroscopy.

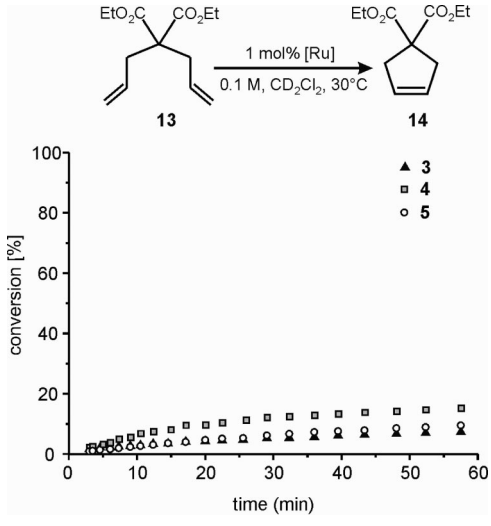

Figure 8. Monitoring RCM of diethyldiallylmalonate by ^{1}H NMR spectroscopy.

dently reported by Herrmann et al., and the influence of these unsaturated NHC ligands on polymer tacticity was explored.[19] The presence of a chiral environment at the metal center has no significant effect on tacticity. This is probably due to the rapid internal rotation of the chiral substituents around the C−N axis that leaves the active chiral space at the metal center relatively ill-defined, hampering the chiral induction. To date, the NHC ligands possessing chiral N-substituents may be efficient as stereodirecting ligands in different reactions if the N-substituents are either sterically demanding or locked in fixed conformations.[20] The combination of chiral N-substituents with chiral N-heterocycles has been studied in enantioselective NHC copper-catalyzed 1,4-conjugate addition reactions. However, matching and mismatching effects were observed.[21]

Scheme 3. CM of Allylbenzene and *cis*-1,4-Diacetoxy-2-butene

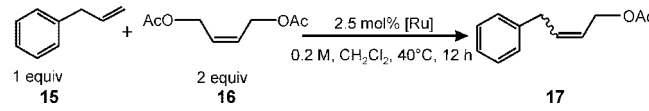

Scheme 4. ARCM of Prochiral Triene

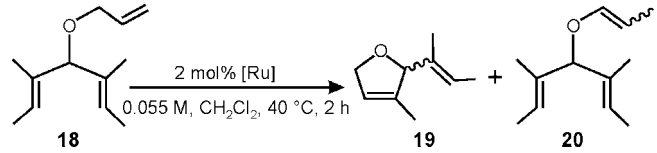

In this framework we decided to compare the behavior of different symmetry complexes (C_2 for **3** and **5** and C_1 for **4**) containing two (**3**) and four (**4** and **5**) stereogenic centers on the NHC ligands in a representative asymmetric ring-closing metathesis reaction, i.e., the desymmetrization of prochiral triene **18** to dihydrofuran **19** (Scheme 4).[8,9] It is worth noting that complexes **4** and **5** differ only in the endocyclic chirality of the NHC: stereogenic centers on the backbone are *R,S* and *R,R* for **4** and **5**, respectively.

(16) Ritter, T.; Hejl, A.; Wenzel, A. G.; Funk, T. W.; Grubbs, R. H. *Organometallics* **2006**, *25*, 5740.
(17) Bielawski, C. W.; Grubbs, R. H. *Angew. Chem.* **2000**, *112*, 3025; *Angew. Chem., Int. Ed.* **2000**, *39*, 2903.
(18) Chatterjee, A. K.; Choi, T. -L.; Sanders, D. P.; Grubbs, R. H. *J. Am. Chem. Soc.* **2003**, *125*, 11360.
(19) (a) Weskamp, T.; Kohl, F. J.; Herrmann, W. A. *J. Organomet. Chem.* **1999**, *582*, 362. (b) Hamilton, J. G.; Frenzel, U.; Kohl, F. J.; Weskamp, T.; Rooney, J. J.; Herrmann, W. A.; Nuyken, O. *J. Organomet. Chem.* **2000**, *606*, 8.
(20) Cesar, V.; Bellemin-Laponnaz, S.; Gade, L. H. *Chem. Soc. Rev.* **2004**, *33*, 619, and references therein.
(21) (a) Guillen, F.; Winn, C. L.; Alexakis, A. *Tetrahedron: Asymmetry* **2001**, *12*, 2083. (b) Alexakis, A.; Winn, C. L.; Guillen, F.; Pytkowicz, J.; Roland, S.; Mangeney, P. *Adv. Synth. Catal.* **2003**, *3*, 345. (c) Winn, C. L.; Guillen, F.; Pytkowicz, J.; Roland, S.; Mangeney, P.; Alexakis, A. *J. Organomet. Chem.* **2005**, *690*, 5672.

Catalyst **3** ring-closed **18** with 66% conversion (entry 10, Table 3) to give the almost racemic product **19**, along with 34% of unwanted isomerization product **20** (*E*:*Z* ~1:1.5). Catalyst **4** showed high activity (100% within 2 h) but no enantiomeric excess (ee) in the desymmetrization of substrate **18** (entry 11, Table 3).

However, when triene **18** was treated with **5** under identical reaction conditions, we observed dihydrofuran **19** in 59% yield and 33% ee *pro R* configuration. Also in this case, 41% of isomerized starting triene was found (*E*:*Z* ~1:1.6) (entry 12, Table 3). Isomerization products are known to be obtained from hydride species formed from the decomposition of ruthenium olefin metathesis catalysts.[22] In order to suppress olefin isomerization during this process, the same reaction was run in the presence of 2,6-dichloro-1,4-benzoquinone.[23] The presence of this additive effectively prevented the unwanted metathetical isomerization, but it had no relevant effect on the yield (60%) and no increase in ee (entry 13, Table 3).

To improve the enantioselectivity, we changed the halide ligands of catalyst **5** from Cl^- to I^- by using NaI as an additive.[8,9] The addition of NaI afforded high conversion (>90%) and at the same time a poor ee (about 7%) *pro S* configuration of **19** (entry 14, Table 3). This result was unexpected both for the higher yield of the desired product and for the inversion of the absolute configuration in the *ee* of the product with respect to entry 12. The higher conversion into the desired product could be due to the increased stability of the I^--substituted catalyst toward the formation of hydride species arising from the decomposition of Ru catalysts. In fact the steric hindrance of I^- could prevent a hydrogen abstraction from the ligand, which tipically leads to a hydride species. The inversion of the absolute configuration, with low but highly reproducible enantiomeric excess, could be correlated to a different arrangement of N-substituents in the presence of the bulky I^-.

The following principal conclusions could be drawn from this study:

• As expected, the presence of only chiral N-substituents as in the NHC ruthenium complex **3** is inefficient in transferring the chiral information to the active site of the catalyst.

• Considering also complexes with a 1,2-dimethylethylenediamine skeleton (**4** and **5**), a low chiral induction is appreciable when the methyls on the backbone of the NHC possess an *anti* stereochemistry.

Conclusions

We reported the synthesis of three novel monodentate Ru-based catalysts presenting chiral NHC ligands (**3**, **4**, and **5**). To the best of our knowledge, these are the first examples of Ru complexes with symmetrical saturated NHC ligands bearing nonaromatic N-substituents. Full NMR characterization in a wide temperature range ($-80 < T < 80$ °C) shows that both **4** and **5** present atropisomers. In particular, at low temperature **4** and **5** are characterized by the presence of four and two different isomers, respectively, while at room temperature the presence of two and one isomer is revealed for **4** and **5**, respectively. According to DFT calculations, the interconversion between different atropisomers, which occurs at room temperature, would be due to the free rotation of the benzylidene group around the Ru=C bond, whereas the isomerization through NHC rotation around the Ru−C bond should not occur in the NMR explored temperature range and time scale, due to the high free energy barrier. These results are supported by the excellent agreement of the free energy activation barrier, estimated by NMR data of complex **5**, and the calculated free energy barrier corresponding to the rotation of the alkylidene group.

The performance of **3**, **4**, and **5** in ROMP, RCM, CM, and ARCM was tested. All three catalysts were able to promote the explored metathesis reactions. **4** exhibited the highest activity in all these metathetic processes. As for ROMP and CM, **3**−**5** showed activities between those of **1** and **2** and gave improved selectivity toward *Z* double-bond formation.[16]

Modest enantioselectivity (33%) in the ARCM of an achiral triene was observed in the presence of **5**. This result is consistent with the C_2 symmetry of the ligand.[8,9] On the other hand, **3**, which has the same ligand symmetry, but without chirality in the backbone, was totally unable to give enantioinduction in ARCM. This result underlines the minor role of the chiral N-substituents in transferring the asymmetric information and the relevance of the chiral substitution of the backbone.

Experimental Section

All reactions involving metal complexes were conducted in oven-dried glassware under nitrogen atmosphere with anhydrous solvents, using standard Schlenk techniques and glovebox techniques. Toluene and THF were distilled from sodium/benzophenone. CH_2Cl_2 and Et_2O were dried on CaH_2 and freshly distilled before use. All chemical products were purchased from Sigma -Aldrich Company and were reagent quality. These products were used without further purification. The syntheses of diamines **4a**, **4b**, and **4c** were effected by reported procedures.[12] Triene **18** was prepared as previously reported.[9] Flash column chromatography of organic compounds was performed using silica gel 60 (230−400 mesh). Silica gel for the purification of organometallic complexes was obtained from TSI Scientific, Cambridge, MA (60 Å, 230−400 mesh, pH 6.5−7.0). Analytical thin-layer chromatography (TLC) was performed using silica gel 60 F254 precoated plates (0.25 mm thickness) with a fluorescent indicator. Visualization of TLC plates was performed by UV light and $KMnO_4$ or I_2 stains. Enantiomeric excesses were determined by chiral GC (Chiraldex G-TA, 30 m × 0.25 mm) and were compared to racemic samples. All deuterated solvents were degassed under an N_2 flow and stored over activated molecular sieves (4 Å) in a glovebox prior to use. NMR spectra were recorded on a Bruker AM300 and Bruker Avance 400 operating at 300 and 400 MHz for ^1H, respectively. The ^1H and ^{13}C chemical shifts are referenced to $SiMe_4$ ($\delta = 0$ ppm) using the residual protio impurities of the deuterated solvents as internal standard. ^{31}P NMR spectra were referenced using H_3PO_4 ($\delta = 0$ ppm) as an external standard. Spectra are reported as follows: chemical shift (δ ppm), multiplicity, coupling constant (Hz), and integration. Multiplicities were abbreviated as follows: singlet (s), doublet (d), triplet (t), quartet (q), multiplet (m), and broad (br). The ^{13}C NMR assignments were confirmed by two-dimensional correlation experiments (HSQC).

General Procedure for the Synthesis of Chiral Rutenium Complexes 3−5. In a glovebox, a 50 mL flask was charged with imidazolinium salt (1.5 equiv), potassium hexafluoro-*tert*-butoxide (1.5 equiv), $(PCy_3)_2Ru(=CHPh)Cl_2$ (1 equiv), and toluene. The reaction tube was sealed with a septum, removed from the glovebox, and heated at 60 °C for 3 h. After cooling, the reaction mixture was concentrated and purified by flash column silica gel chromatography to afford the desired ruthenium catalyst as a powder.

Ruthenium Compound 3. Following the general procedure above, **9** (250 mg, 0.68 mmol), potassium hexafluoro-*tert*-butoxide (150 mg, 0.68 mmol), and $(PCy_3)_2Ru(=CHPh)Cl_2$ (375 mg, 0.45 mmol) in 6 mL of toluene afforded 130 mg (35%) of a pinkish-brown powder (10% Et_2O in pentane).

^1H NMR (400 MHz, CD_2Cl_2): δ 20.04 (s, Ru=C*H*Ph), 8.51 (br s), 7.87 (d), 7.50−7.13 (m), 6.10 (q), 4.74 (q), 3.50−3.44 (m) 3.13 (m), 2.99 (m), 2.45 (q), 1.96 (d), 1.72−0.87 (several peaks). ^{13}C NMR

(22) Hong, S. H.; Day, M. W.; Grubbs, R. H. *J. Am. Chem. Soc.* **2004**, *126*, 7414.

(23) Hong, S. H.; Sanders, D. P.; Lee, C. W.; Grubbs, R. H. *J. Am. Chem. Soc.* **2005**, *127*, 17160.

(100 MHz, CD_2Cl_2): δ 291.1 (s, Ru=*C*HPh), 217.5 (d, J(P,C) = 70,6 Hz, *i*N*C*N), 153.0, 140.3, 139.7, 130.8, 129.5, 128.8, 128.6, 128.4, 128.3, 127.7, 56.7, 56.0, 44.0, 43.5, 32.2, 32.0, 29.8, 29.7, 28.23, 28.16, 26.9, 17.1, 16.9. ^{31}P NMR (161.97 MHz, CD_2Cl_2): 39.0 ppm. Anal. Calcd (%) for $C_{44}H_{62}Cl_2N_2PRu$ (820.92): C 64.38, H 7.49, N 3.41. Found: C 64.12, H 7.50, N 3.35.

Ruthenium Compound 4. Following the general procedure above, **10** (450 mg, 1.14 mmol), potassium hexafluoro-*tert*-butoxide (250 mg, 1.14 mmol), and $(PCy_3)_2Ru(=CHPh)Cl_2$ (628 mg, 0.76 mmol) in 8 mL of toluene afforded 290 mg (45%) of a brown powder (5% to 10% Et_2O in pentane). ^{1}H NMR (400 MHz, CD_2Cl_2) for a mixture of atropisomers (2.7:1): δ 20.03 (s, major isomer, 19.93 minor isomer Ru=C*H*Ph), 8.52 (br m), 8.02 (d), 7.93 (d), 7.52−7.06 (m), 6.01 (m), 4.86 (br s), 4.20−3.69 (several peaks), 3.21 (br s), 2.49−0.87 (several peaks), 0.51 (d), 0.43 (d). ^{13}C NMR (100 MHz, CD_2Cl_2): δ 290.4 (d, J(P,C) = 7.03 Hz, Ru=*C*HPh), 218.6 (broad signal, *i*N*C*N), 153.0, 142.3, 142.1, 140.1, 139.5, 139.5, 129.5, 129.1, 128.9, 128.8, 128.2 (two overlapped peaks), 128.1, 127.9, 59.1, 58.3, 58.0, 57.7, 57.1, 56.5, 55.7, 32.4, 32.2, 30.0, 29.7 (two overlapped peaks), 28.3, 28.2, 28.1, 27.0, 20.1, 19.5, 18.9, 15.6, 14.6, 14.2. ^{31}P NMR (161.97 MHz, CD_2Cl_2): δ 39.5 ppm (broad signal). Anal. Calcd (%) for $C_{46}H_{66}Cl_2N_2PRu$ (848.97): C 65.08, H 7.72, N 3.30. Found: C 65.00, H 7.62, N 3.26.

Ruthenium Compound 5. Following the general procedure above, **11** (450 mg, 1.14 mmol), potassium hexafluoro-*tert*-butoxide (250 mg, 1.14 mmol), and $(PCy_3)_2Ru(=CHPh)Cl_2$ (628 mg, 0.76mmol) in 8 mL of toluene afforded 258 mg (40%) of a brown powder (5% to 10% Et_2O in pentane). ^{1}H NMR (400 MHz, CD_2Cl_2): δ 19.92 (s, Ru=C*H*Ph), 8.41 (br s), 8.01 (d,), 7.45−7.16 (m), 6.07 (q), 5.03 (br m), 3.48 (br s), 3.32 (br s), 2.41 (q), 2.00 (d), 1.85−0.47 (several peaks). ^{13}C NMR (75 MHz, CD_2Cl_2): δ 289.8 (d, J(P,C) = 5.95 Hz, Ru=*C*HPh), 217.5 (d, J(P,C) = 69,79 Hz, *i*N*C*N), 153.1, 141.8, 141.6, 131.5, 130.9, 129.4, 129.2, 128.5, 128.3, 127.7, 127.4, 62.13, 57.0, 55.7, 32.4, 32.2, 30.3, 29.8, 29.7, 28.3, 28.1, 26.9, 20.2, 17.0. ^{31}P NMR (161.97 MHz, CD_2Cl_2): δ 39.7 ppm. Anal. Calcd (%) for $C_{46}H_{66}Cl_2N_2PRu$ (848.97): C 65.08, H 7.72, N 3.30. Found: C 64.97, H 7.70, N 3.27.

ROMP of COD (12, Figure 7, Table 3). An NMR tube with a screw-cap septum top was charged with 0.80 mL of a CD_2Cl_2 solution of catalyst (0.40 μmol). After equilibrating at 30 °C the sample in the NMR probe, 49.1 μL (0.40 mmol) of **12** was injected into the tube. The polymerization was monitored as a function of time, and the conversion to poly(**12**) was determined by integrating the methylene protons in the starting monomer, δ 2.36 (m), and those in the product, δ 2.09 (br m), 2.04 (br m).

RCM of Diethyldiallylmalonate (13, Figure 8, Table 3). An NMR tube with a screw-cap septum top was charged with 0.80 mL of a CD_2Cl_2 solution of catalyst (0.80 μmol). After equilibrating at the appropriate temperature the sample in the NMR probe, 19.3 μL (0.080 mmol) of **13** was injected into the tube. The reaction was monitored as a function of time, and the conversion to **14** was determined by integrating the methylene protons in the starting monomer, δ 2.61 (dt), and those in the product, δ 2.98 (s).

CM of Allylbenzene (15) and *cis*-(1,4)-Diacetoxy-2-butene (16) (Scheme 2, Table 3). A 55 μL portion of **15** (0.5 mmol) and 160 μL of **16** (1.0 mmol) were added simultaneously via syringe to a stirring solution of catalyst (0.013 mmol) in 2.5 mL of CH_2Cl_2. The flask was refluxed under nitrogen for 12 h. The reaction mixture was concentrated and purified directly on a silica gel column (9:1 hexane/ethylacetate). **17** was obtained as a pale oil. *E:Z* ratio was determined by integration of peaks at δ 4.73 and 4.55.

General Procedure for ARCM of Achiral Triene 18 (Scheme 3, Table 3). A 20 mg (0.11 mmol) sample of triene **18** was added to a solution of catalyst (0.27 mmol) in CD_2Cl_2 (2 mL), and the reaction was stirred at 40 °C for 2 h. The conversion to the desired cyclic product **19** was determined by comparing the ratio of the integrals of the prochiral proton in the starting material, δ 3.94 (br s), with the one in the product, δ 4.88 (br s). The enantiomeric purity was determined after purification of the reaction mixture (5% Et_2O in pentane).

Computational Details. Density functional calculations were performed on all the systems with the Gaussian03 set of programs.[24] BP86 was used as a functional, and gradient corrections were taken from the work of Becke and Perdew.[25−27] The electronic configuration of the molecular systems was described by the split-valence basis set with polarization functions of Ahlirchs and co-worker (standard SVP basis set in Gaussian03), for H, C, N, O, and Cl. [28] For Ru we used the small-core, quasi-relativistic Stuttgart/Dresden effective core potential (standard SDD basis set in Gaussian03) basis set, with an associated (8s7p6d)/[6s5p3d] valence basis set contracted according to a (311111/22111/411) scheme.[29−31] Minimum free energy structures and transition states were characterized by the presence of zero and one imaginary frequency only, corresponding to the rotation around θ and ϕ. Solvent effects including contributions of nonelectrostatic terms have been estimated in single-point calculations on the gas-phase-optimized structures, based on the polarizable continuous solvation model, PCM. CH_2Cl_2 and toluene were chosen as model solvents.

Acknowledgment. The authors thank Patrizia Oliva and Dr. Mariagrazia Napoli of the Department of Chemistry of University of Salerno for their technical assistance. Financial support from the "Ministero dell'Università e della Ricerca Scientifica e Tecnologica" (PRIN 2004) is gratefully acknowledged. Prof. A. Zagari (Dept. of Biological Sciences and CNISM, Naples) is gratefully acknowledged for providing access to the Rigaku Saturn 944 diffractometer at the Istituto di Biostrutture e Bioimmagini (IBB), CNR, Naples. Mr. G. Sorrentino (IBB-CNR) and Mr. M. Amendola (IBB-CNR) are kindly acknowledged for technical assistance during the X-ray diffraction measurements.

Supporting Information Available: Further synthetic details, X-ray crystallographic data, and Cartesian coordinates and energies of calculated structures. This material is available free of charge via the Internet at http://pubs.acs.org or from the authors.

OM800459Y

(24) Frisch, M. J.; Trucks, G. W.; Schlegel, H. B.; Scuseria, G. E.; Robb, M. A.; Cheeseman, J. R.; Montgomery, J. J. A.; Vreven, T.; Kudin, K. N.; Burant, J. C.; Millam, J. M.; Iyengar, S. S.; Tomasi, J.; Barone, V.; Mennucci, B.; Cossi, M.; Scalmani, G.; Rega, N.; Petersson, G. A.; Nakatsuji, H.; Hada, M.; Ehara, M.; Toyota, K.; Fukuda, R.; Hasegawa, J.; Ishida, M.; Nakajima, T.; Honda, Y.; Kitao, O.; Nakai, H.; Klene, M.; Li, X.; Knox, J. E.; Hratchian, H. P.; Cross, J. B.; Adamo, C.; Jaramillo, J.; Gomperts, R.; Stratmann, R. E.; Yazyev, O.; Austin, A. J.; Cammi, R.; Pomelli, C.; Ochterski, J. W.; Ayala, P. Y.; Morokuma, K.; Voth, G. A.; Salvador, P.; Dannenberg, J. J.; Zakrzewski, V. G.; Dapprich, S.; Daniels, A. D.; Strain, M. C.; Farkas, O.; Malick, D. K.; D. Rabuck, A.; Raghavachari, K.; Foresman, J. B.; Ortiz, J. V.; Cui, Q.; Baboul, A. G.; Clifford, S.; Cioslowski, J.; Stefanov, B. B.; Liu, G.; Liashenko, A.; Piskorz, P.; Komaromi, I.; Martin, R. L.; Fox, D. J.; Keith, T. M.; AlLaham, A.; Peng, C. Y.; Nanayakkara, A.; Challacombe, M.; Gill, P. M. W.; Johnson, B.; Chen, W.; Wong, M. W.; Gonzalez, C.; Pople, J. A. *Gaussian 03, B.1*; Gaussian, Inc.: Pittsburgh, PA, 2003.

(25) Becke, A. *Phys. Rev. A* **1988**, *38*, 3098.

(26) Perdew, J. P. *Phys. Rev. B* **1986**, *33*, 8822.

(27) Perdew, J. P. *Phys. Rev. B* **1986**, *34*, 7406.

(28) Schaefer, A.; Horn, H.; Ahlrichs, R. *J. Chem. Phys.* **1992**, *97*, 2571.

(29) Haeusermann, U.; Dolg, M.; Stoll, H.; Preuss, H. *Mol. Phys.* **1993**, *78*, 1211.

(30) Kuechle, W.; Dolg, M.; Stoll, H.; Preuss, H. *J. Chem. Phys.* **1994**, *100*, 7535.

(31) Leininger, T.; Nicklass, A.; Stoll, H.; Dolg, M.; Schwerdtfeger, P. *J. Chem. Phys.* **1996**, *105*, 1052.